SCIENTIFIC REPORTS

OPEN

SUBJECT AREAS:
MATERIALS
NANOBIOTECHNOLOGY
MOLECULAR BIOLOGY
NANOPHOTONICS

Received
30 August 2011

Accepted
5 January 2012

Published
2 February 2012

Correspondence and requests for materials should be addressed to A.M. (mershin@mit.edu)

Self-assembled photosystem-I biophotovoltaics on nanostructured TiO_2 and ZnO

Andreas Mershin[1], Kazuya Matsumoto[2], Liselotte Kaiser[2], Daoyong Yu[2], Michael Vaughn[3], Md. K. Nazeeruddin[4], Barry D. Bruce[3], Michael Graetzel[4] & Shuguang Zhang[2]

[1]Center for Bits and Atoms, NE47-383, Massachusetts Institute of Technology, 77 Massachusetts Ave. Cambridge, MA 02139, USA, [2]Laboratory for Molecular Self-Assembly, NE47-379, Massachusetts Institute of Technology, 500 Technology Square, Cambridge, MA 02139, USA, [3]Biochemistry, Cellular and Molecular Biology & Chemical and Biomolecular Engineering, 226 Hesler Biology Bldg., University of Tennessee at Knoxville, TN 37996, USA, [4]Laboratory for Photonics and Interfaces (Institute of Chemical Science and Engineering), Ecole Polytechnique Federale de Lausanne, Lausanne, CH-1015, Switzerland.

The abundant pigment-protein membrane complex photosystem-I (PS-I) is at the heart of the Earth's energy cycle. It is the central molecule in the "Z-scheme" of photosynthesis, converting sunlight into the chemical energy of life. Commandeering this intricately organized photosynthetic nanocircuitry and re-wiring it to produce electricity carries the promise of inexpensive and environmentally friendly solar power. We here report that dry PS-I stabilized by surfactant peptides functioned as both the light-harvester and charge separator in solar cells self-assembled on nanostructured semiconductors. Contrary to previous attempts at biophotovoltaics requiring elaborate surface chemistries, thin film deposition, and illumination concentrated into narrow wavelength ranges the devices described here are straightforward and inexpensive to fabricate and perform well under standard sunlight yielding open circuit photovoltage of 0.5 V, fill factor of 71%, electrical power density of 81 μW/cm^2 and photocurrent density of 362 μA/cm^2, over four orders of magnitude higher than any photosystem-based biophotovoltaic to date.

PS-I precisely orchestrates 96 chlorophyll molecules with electron donors and acceptors[1] (**Fig 1 a**) achieving efficient coherent energy transfer[2] and near-unity charge separation quantum yield at ambient temperatures[3,4]. This is a feat unmatched by any man-made photoelectronic device and has led to PS-I being studied as a candidate for many nanobioelectronic applications[5–8], as well as being the original inspiration behind the dye-sensitized solar cell (DSC)[9]. So far, research on PS-I biophotovoltaics has focused on proof-of-principle devices, studying immobilized PS-I complexes and isolated reaction centers (RC) in self-assembled monolayers (SAMs) on flat electrodes[5–8].

Two main obstacles hinder biophotovoltaics from being a more widely studied technology, constantly improved by many independent researchers. Firstly, while extracting PS-I from a variety of abundant sources is easy, drying this extract on electrodes results in rapid loss of function due to denaturation. Secondly, the electrical power output of biophotovoltaics to date has been so low[5–8], that they were of little practical interest and the characterization necessary to improve their performance required cumbersome, expensive to iterate-optimize methods. For instance, in order to obtain measureable photocurrents it was necessary to make up for the low absorption cross sections of the nearly transparent active SAMs. In prior studies this was addressed by using either laser light with power equivalent to 100 times that of standard air-mass 1.5 (AM1.5) sunlight[5], or incoherent monochromatic light[6] in both cases precisely tuned to the pigment absorption maxima –an unrealistic emulation of real-world conditions requiring elaborate instrumentation.

Results

We have removed these two obstacles by designing a PS-I biophotovoltaic whose IV characteristics can be easily studied under regular sunlight and its design and fabrication are amenable to low-cost, iterative optimization. To avoid denaturation, we treated PS-I with designer peptide surfactants[1]. To improve photovoltaic performance we increased the light absorption cross-section without changing the footprint by departing from the traditional flat

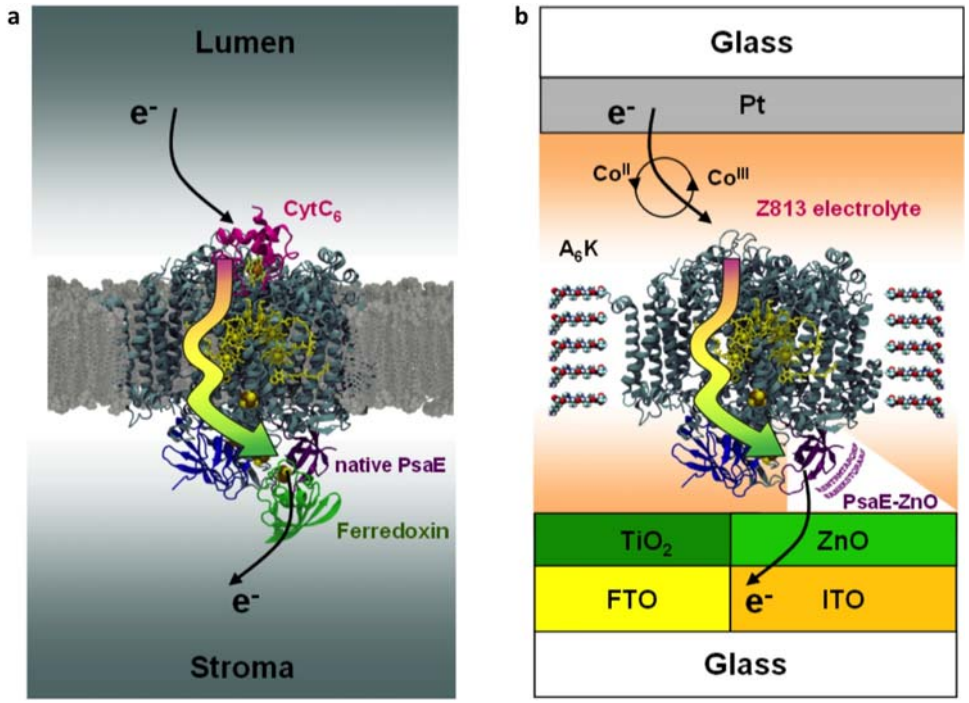

Figure 1 | Schematic of PS-I in cellular membrane and in two types of biophotovoltaic cells. (a) PS-I in ~30Å thick cellular bilipid membrane (grey). Arrows indicate direction of electron travel with acceptor side facing down. The core subunits are shown in grey and the only prosthetic groups are the core electron transport associated cofactors including the P700 chlorophyll (Chl) dimer in the center, the four associated Chl a molecules (green), the two phyloquinone acceptors (orange), and the three FeS centers Fx, Fa and Fb (yellow) (sulfur) and brown (Fe). The ribbon diagram of stromal subunits PsaD, PsaC, and PsaE is shown protruding outside of the membrane and colored blue, red, and purple respectively. (b) The natural redox mediators cytochrome c and ferredoxin are absent, replaced by Z813 electrolyte and either a TiO_2 nanocrystalline sintered paste (left) or ZnO nanowires (right). Left: stabilized PS-I physisorbed to TiO_2 on fluorine-doped tin oxide (FTO) coated glass. Right: (bioengineered) PS-I self-assembled in the presence of an overabundance of PsaE-ZnO subunit on ZnO nanowires grown on ITO glass. In both cases, energy levels are matched to favor electron transfer from electrolyte to photoanode[5–8].

electrode geometry in favor of mesoscopic, high-surface area semiconducting electrodes (TiO_2 nanocrystals and ZnO nanowires). Finally, we showed how high affinity peptide motifs[10] bioengineered to promote selective adsorption to specific substrates can enhance photovoltaic performance. These materials, geometries and design resulted in simple, robust biophotovoltaic devices of unprecedented performance.

Photochemically active, trimeric PS-I was isolated and characterized from the thylakoids of the thermophilic cyanobacteria *Thermosynechococcus elongatus* as described in detail in Fig. 2 of Iwuchukwu *et al.*[11]. This PS-I was stabilized for several months in solution[12] and in dry form by designer peptide surfactants[1] **(Fig. 2)**. To build devices, PS-I molecules were air-dried on nanostructured semiconducting substrates and the circuits were completed by liquid electrolyte and platinized glass as is common for conventional DSCs **(Fig. 1 b).** We used nanocrystalline TiO_2 and ZnO nanowires to provide a large effective surface area (A_{eff}) for PS-I adsorption and light harvesting **(Fig. 3)** and without any further optimization, these devices achieved electrical power outputs P_{out} of up to 81 μW/cm^2 and area-normalized short-circuit current densities I_{sc}^{Norm} of up to 362 μA/cm^2 **(Fig. 4)**. These parameters are to be compared to the over 10,000 times lower I_{sc}^{Norm} (~30 nA/cm^2) reported previously with monochromatic illumination tuned to the ~800 nm absorption peak of a monolayer of PS-I on a thin film of gold (actual power efficiency not reported)[7] and to the up to 120 μA/cm^2 I_{sc}^{Norm} observed when isolated RCs were chemically bound to a series of evaporated metallic and semiconducting thin films and illuminated with 10 W/cm^2 laser light (one-hundred times the power density of AM1.5 sunlight) all concentrated into the 808 nm absorption peak of RCs[5]. While there have been various estimated and theoretical maximum efficiencies (e.g. an upper possible limit of 20% efficiency for RC-biophotovoltaics[5]), there have been no reports of conversion efficiency η for PS-I (where $\eta = \frac{P_{out}}{P_{in}}$, P_{in} the total power of the incident light and P_{out} the total resulting electrical power). Our photocurrent measurements were carried out under AM1.5 standard simulated sunlight with precisely controlled active surface areas (0.159 cm^2) and continuously-calibrated, spectral-mismatch corrected sunlamps, as is the standard in the conventional photovoltaic industry[13]. Under these conditions, that closely emulate outdoor sunlight, the total external efficiency of conversion of incident sunlight to useable electricity was $\eta \sim 0.08\%$. This must not to be confused with the sometimes very high quantum or internal efficiencies routinely reported for organic optoelectronics.

PS-I Biophotovoltaic Solar Cell. In photosynthetic organisms, PS-I catalyses light-driven electron transfer from reduced plastocyanin located in the lumen, to ferredoxin in the stroma providing a path across the membrane consisting of a chain of cofactors (**Fig. 1a**). Light absorption results in excitation of the primary electron donor (P700), transfer to primary and secondary electron acceptors and finally crossing of the membrane. In our biophotovoltaic solar cell, the role of plastocyanin was played by the Co(II)/Co(III) ion-containing electrolyte Z813[14], and ferredoxin was replaced by either nanocrystalline TiO_2 (**Fig. 1 b left**) or ZnO-nanowires (**Fig. 1 b right**) to provide large-surface area electron acceptors.

When using TiO_2, we chose the pore size of the nanocrystalline film to be double the diameter of our PS-I particles to ensure a high probability of physisorption. When using ZnO nanowires, we substituted (by a self-assembly exchange reaction) the naturally-occurring electron acceptor PsaE subunit with one that contained an amino acid sequence with high affinity for ZnO: RSNTRMTARQHRSANHKSTQRARS[10]

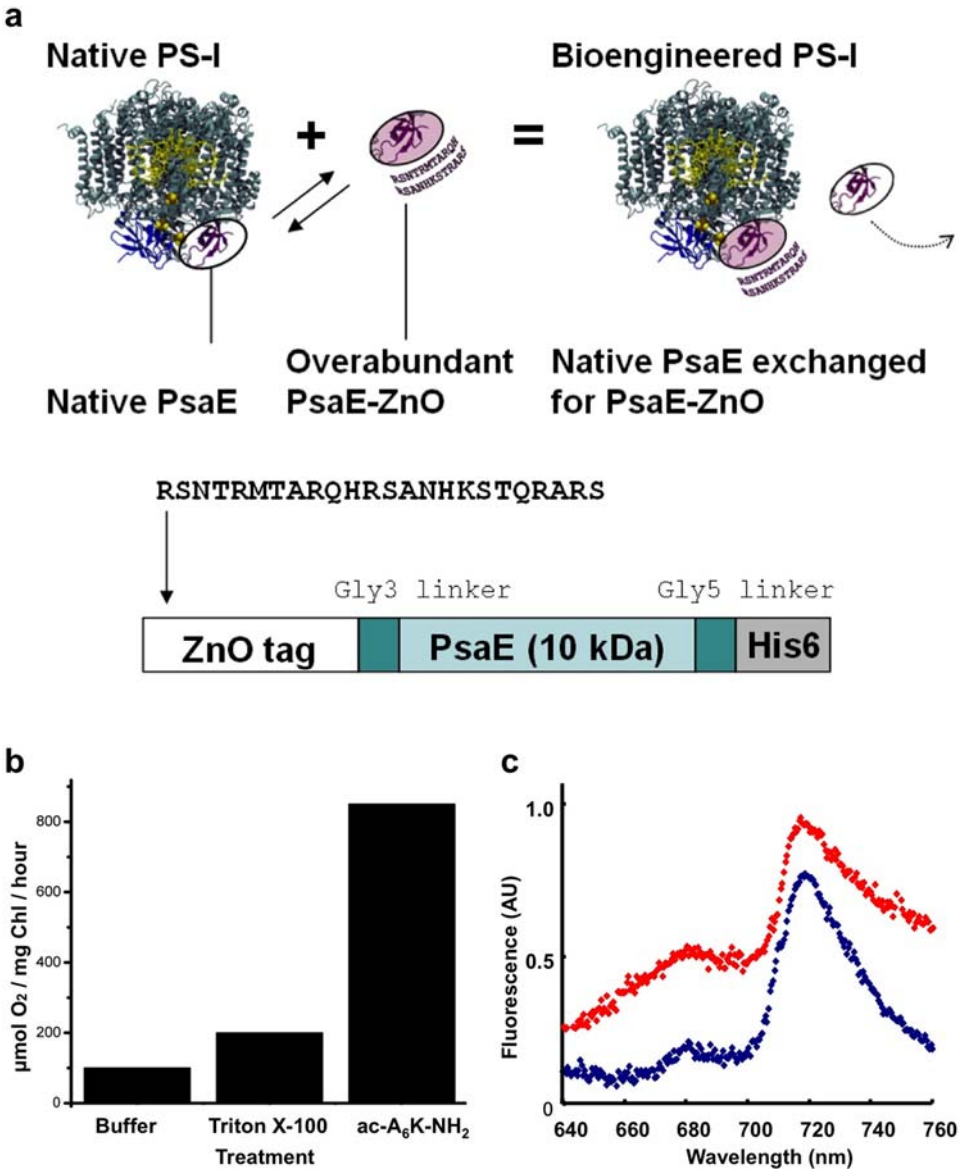

Figure 2 | (a) To promote attachment and orientation of the entire PS-I complex to ZnO nanowires, we fused the ZnO-binding peptide tag RSNTRMTARQHRSANHKSTQRARS[10] (expressed in E.coli) to the N-terminus of the PsaE subunit. Upon exchanging native PsaE in favor of PsaE-ZnO and self-assembly, the modified PS-I preferentially binds to ZnO nanowires by the electron acceptor side, minimizing distance between electron acceptor and electrode and maximizing electron transfer. (b) The marked increase in the rate of methyl viologen (MV)-mediated oxygen reduction by PS-I in the presence of the designer surfactant peptide A_6K, indicates that A_6K maintains the ability of PS-I to catalyze photochemical charge separation and MV-mediated O_2 uptake relative to the control treatment with either the non-ionic detergent Triton X-100 (middle) or DDM present in the isolation buffer (left). Increased O_2 uptake activity cannot be due to free chlorophyll-mediated O_2 consumption (via^{3}chl) since treating cyanobacterial PS-I with strong detergents (1% SDS) leads to only minimal loss of chlorophyll from PS-I[22]. All activity tests are normalized per mol of PS-I. (c) Low-temperature fluorescence of PS-I self-assembled in the presence of excess PsaE-ZnO (red) peaks at the same two wavelengths as unaltered PS-I extract (blue) indicating that bulk chlorophyll organization is preserved[12] and the stabilizing interaction with A_6K is likely similar in both cases.

(PsaE-ZnO) thus promoting adhesion and minimizing the distance that electrons must travel to the anode (**Fig. 2 a**).

Stabilization of Native and Bioengineered PS-I. Stabilization of dry PS-I extract on glass and on the transparent conductor Indium-Tin-Oxide (ITO) for at least three weeks has been described elsewhere[1]. Here, we mixed PS-I at 0.4 mg/mL in a 1 : 1 ratio with 0.1% (w/v) of the 2.4 nm long cationic peptide surfactant Ac-AAAAAAK-NH_2 (A_6K) consisting of six alanines and a lysine at the amidated C-terminus and observed enhanced stability (**Fig. 2 b**). The bioengineered, self-assembled PS-I containing PsaE-ZnO exhibited low-temperature fluorescence peaks identical to unmanipulated PS-I extract undergoing identical treatment (**Fig. 2 c**), indicating that subunit substitution did not adversely affect structure and we expect the photochemical-activity enhancing effect of A_6K to be similar in both cases.

Nanocrystalline TiO_2 and ZnO Nanowires as Large Surface Area Photoanodes. I_{sc} is directly proportional to electrical power output and is controlled by light absorption. To increase the useful light incidence angle and optical cross-section of our biophotovoltaics, we used two types of rough, large surface area semiconductors as photoanodes. This made our devices able to absorb light from nearly a 2π solid angle and provided an increased effective area for PS-I

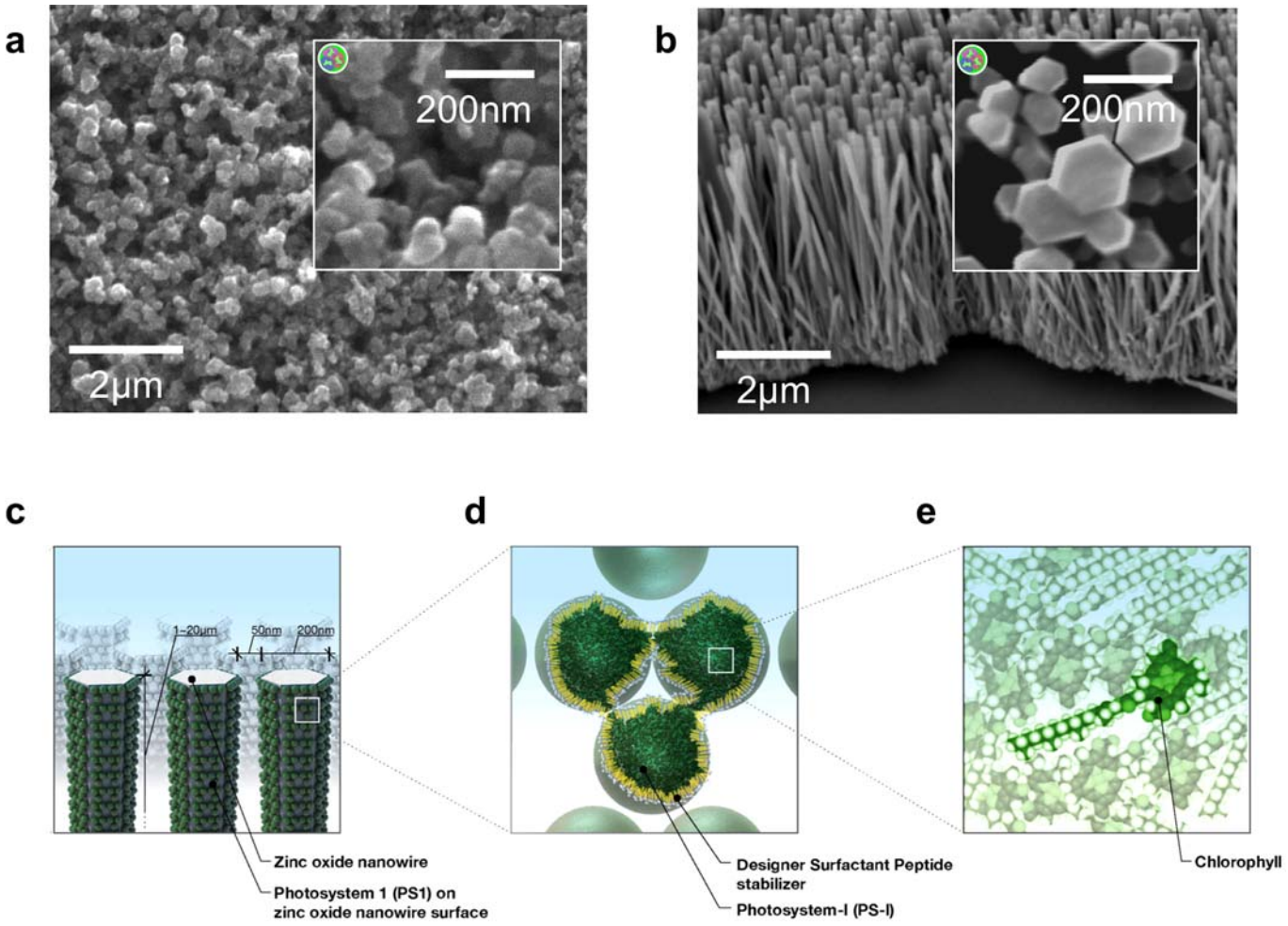

Figure 3 | SEM of nanostructured TiO_2 and ZnO photoanodes and schematic of an ideal ultra-low cost biophotovoltaic arrangement. (a) 3.8 μm-thick, 60 nm-pore TiO_2 nanocrystalline photoanode of roughness factor ρ_{TiO2} ~200 (i.e. surface area increases by roughly fifty times per μm of film thickness) fabricated as described previously[13]. (b) 3 μm tall, ZnO nanowires grown on Zn-nanoparticle-seeded ITO-glass as described elsewhere[15], ρ_{ZnO}~30. Round graphic at top left of inserts represents a PS-I trimer drawn to scale. (c), (d), (e) ideal arrangement of PS-I and designer surfactant peptide stabilizers on ZnO nanowires that could be grown at room temperature on a variety of flexible and inexpensive substrates[16].

SAM adsorption: A_{eff} ~200 times that of the flat footprint for TiO_2 nanocrystals (Fig 3 a) and ~30 times with ZnO nanowires (Fig 3 b). In addition to providing an inexpensive alternative to TiO_2, the charge carrier mobility of ZnO nanowires is one-hundred times faster than TiO_2[15] and large-scale, ambient temperature solution-growth of ZnO nanowires is simple, requiring fewer steps, less energy and is easily adaptable to flexible conducting substrates[16]. However, ZnO DSC photoanodes have so far always under-performed[15] when compared with identically sensitized TiO_2. This is due to their lower roughness factor ρ, poor dye loading, and the shunting of the photocurrent by the corrosion of ZnO by common DSC dyes and electrolytes. The IV behavior of our biophotovoltaics indicated that tagging PS-I with an amino acid sequence that binds to ZnO promoted orientation and/or binding to ZnO nanowires with $\eta = 0.03\%$, for PsaE-ZnO, while $\eta = 0.00\%$ for the histidine-tagged control (Fig. 4 d and e respectively). The I_{sc} achieved with ZnO (Fig. 4 d) is roughly a factor of ten lower than that with TiO_2, consistent with the ratio of the two A_{eff} (ρ_{ZnO}~30, ρ_{TiO2}~200) suggesting that A_{eff} is the primary control of I_{sc}.

Photocurrent Measurements Under Realistically Simulated Solar Illumination. The shapes of the IV curves (**Fig. 4**) obtained upon exposing our devices to AM1.5 sunlight for both PS-I complexes on TiO_2 and bioengineered PS-I on ZnO are similar to conventional DSCs. After accounting for the UV-excited photocurrent (**Fig. 4b**) the following four types of control devices, containing all buffer components and electrolyte, did not yield any additional photovoltaic action: i) devices made with denatured PS-I (boiled for 10 min), ii) blanks without PS-I or A_6K , iii) blanks without PS-I but with A_6K, iv) devices with PS-I but no A_6K. This leaves stabilized, non-denatured PS-I as the only possible agent behind 80% of the maximum measured photocurrent (the remaining 20% being due to UV excitation of TiO_2 and ZnO). We emphasize that these photocurrents cannot be attributed to sensitization by leached chlorophyll, because unless precisely organized by the PS-I scaffold, chlorophyll alone does not act as a photovoltaic sensitizer[1], the interaction between the chlorophyll ester units with the TiO_2 surface is weak and chlorophyll does not adsorb[17] on TiO_2 or ZnO .

Discussion

Using inexpensive raw materials and simple processes, we have achieved record biophotovoltaic performances. We isolated PS-I from thermophilic cyanobacteria, but the structural similarity between this and higher plant PS-I suggests that many other

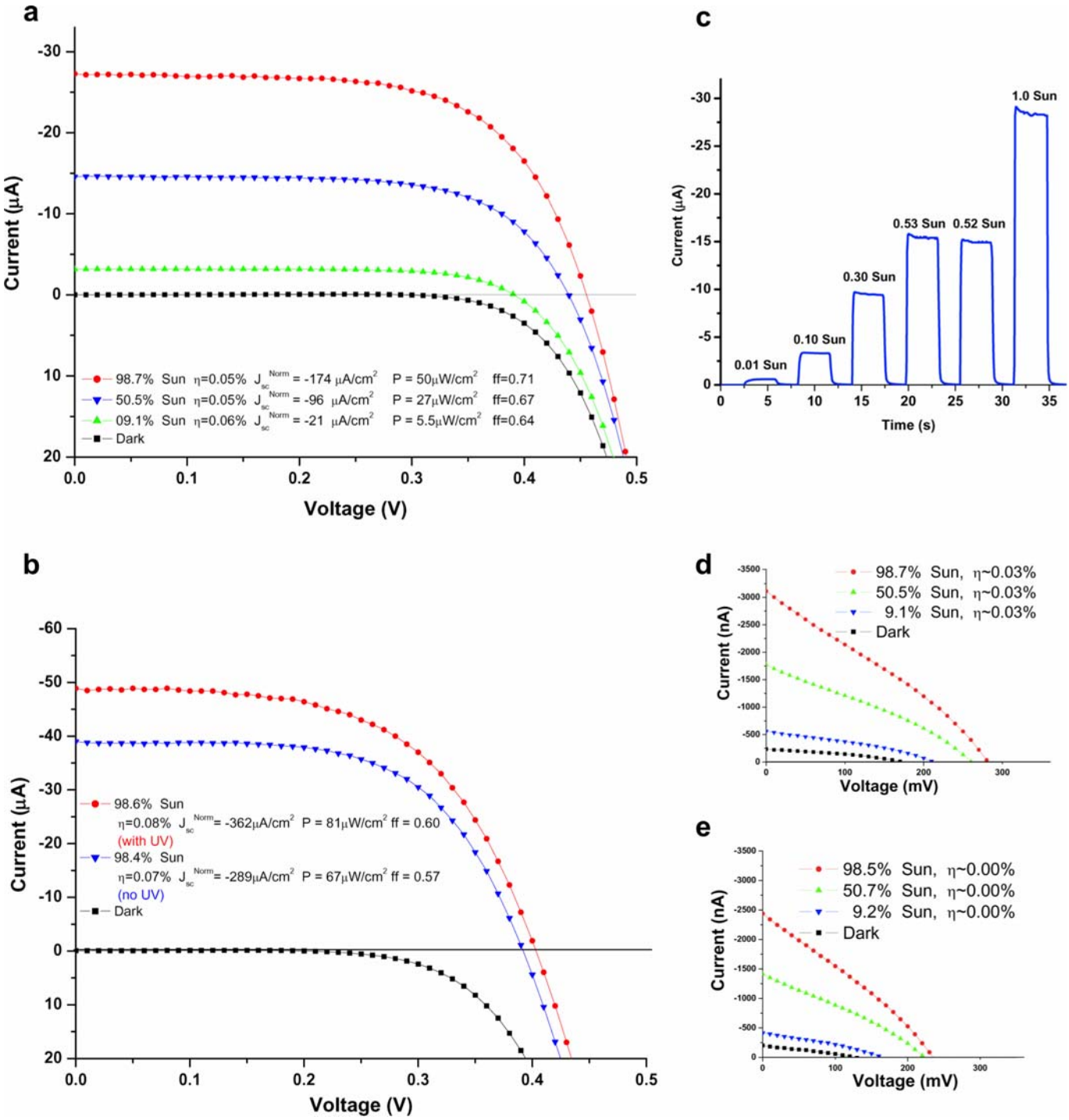

Figure 4 | Photocurrent measurements of PS-I biophotovoltaic devices under AM1.5 simulated insolation at 298°K. Illuminated surface 0.159 cm^2 (a) 40 μl of PS-I (0.2 mg/mL) stabilized by 1 : 1 0.1%w/v designer surfactant peptide A_6K (resulting in a total of 8 μg of protein) dried on a 3.8 μm thick layer of 60 nm-pore TiO_2 produces an IV curve typical of a DSC. Fill factor (ff) ranged from 64% to 71% (b) Eliminating ultraviolet (UV) wavelengths below 350 nm resulted in a ~20% reduction in the normalized short circuit current (J_{sc}^{Norm}) and a ~10% reduction in the open circuit voltage (V_{oc}) indicating that 80% of the total electrical power generated is due to PS-I (the rest due to UV photovoltaic response of TiO_2). These photocurrents cannot be attributed to sensitization of TiO_2 by leached chlorophyll derivatives[1,17]. A blank control containing A_6K generated no power when exposed to UV-less sunlight of any intensity, neither did controls built with PS-I denatured by boiling for 10 minutes, nor devices built with PS-I not treated with A_6K (data not shown). Total incident-light to electrical external power conversion efficiency η was 0.08% with UV, 0.07% without. (c) Linearity test of PS-I photocurrent at intensities from 0.01x to 1.0x AM1.5 shows behavior typical of a DSC. (d) IV of PS-I self-assembled in the presence of an overabundance of PsaE-ZnO electron-accepting subunit yields a total power conversion efficiency, η=0.03%. (e) Control: IV of PS-I self-assembled with an overabundance of non-ZnO specific histidine-tag containing PsaE subunit yields lower V_{oc}, J_{sc}^{Norm} and η=0.00% as expected, suggesting that the PsaE-ZnO tag either enhanced binding of PS-I to the ZnO nanowires or favored the optimal orientation, or both. Z813 Co(II)/Co(III) electrolyte[14] and platinized glass were used to complete all devices.

abundant sources of highly pigmented thylakoids can also be used including the normally discarded leafy parts of common agricultural crops or timber. PS-I is indeed a promising raw material for ultra-low-cost biophotovoltaics as postulated by LaVan *et al.*[4] but significant optimization challenges must be met. The devices characterized here indicate merely the lowest limit of PS-I biophotovoltaic performance possibilities. Since we did not perform any optimization, significant efficiency gains can be expected from increased loading, better oriented and more tightly coupled PS-I to photoanode, customization of stabilizing agents and better matching of bio-friendly electrolytes with photoanode/photocathode substrates. The short-term stability and photoactivity of various treatments of PS-I is summarized in **Fig. 2 b** and discussed in detail elsewhere[1,12] and is encouraging. Clearly, tracking biophotovoltaic performance over the long-term is an important future step but was beyond the scope of the present study[18]. While we used centrifugation, equally pure PS-I can be isolated from plant or bacterial extracts by porous membrane bioseparation, an inexpensive method that can be scaled up to industrial levels by simple yet highly efficient affinity binding with protein-specific epitope tags[19]. The design and methodology principles described here are suitable to biophotovoltaics that can be characterized under ordinary sunlight. We hope these results encourage optimization efforts to deliver biosolar power that is truly "green".

Methods

Cloning and expression of ZnO-binding subunits. While we here show data on PsaE only (**Fig. 2c**), plasmids coding for PsaE (UniProt accession number Q62007) and also PsaD (UniProt accession number P34982) from *Cyanobacterium Mastigocladus laminosus* were expressed and studied. Both self-assemble near the final electron acceptor and ejection site of the PS-I complex and are ideally placed to appropriately attach and orient the molecule to a photoanode. The peptide tag RSNTRMTARQHRSANHKSTQRARS[10], was fused to the N-terminal of the respective coding sequence via a five-residue glycine linker and a six residue histidine tag was fused to the C-terminal by PCR **(Fig. 2a)** and cloned into expression plasmid pET-DEST42, Invitrogen (Carlsbad, CA, USA), according to the manufacturer's instructions. The plasmids were transformed into the *Escherichia coli (E. coli)* expression strain BL21 (*DE3*) pLysS. Protein expression was carried at 37°C in LB media and the soluble protein fraction isolated by centrifugation after lysing cells by sonication. The proteins were purified using His-Trap column (GE Healthcare, Uppsala, Sweden) using an ÄKTA purifier chromatography system (GE Healthcare), according to the manufacturer's instructions.

Subunit exchange. To exchange the native PsaE (or PsaD) in PS-I to the recombinant PsaE-ZnO (or PsaD-ZnO), the recombinant proteins were incubated with PS-I in a 50 : 1 molar ratio for 2 hours at 4°C. Free PsaE (or PsaD) was removed by centrifuging the sample over an YM-100 filter (Millipore) leaving unbound PsaE (or PsaD) in the flow-through (**Fig. 2a**). These exchange reaction protocols are expected to yield exchange efficiency of >65%. Since we used a dual isolation system using both IMAC and sucrose density exchange, we know with certainty that our efficiency is higher than 65%.

Stability test of immobilized PS-I via low temperature fluorescence spectroscopy. Low-temperature fluorescence spectroscopy[1] was used to ascertain stability of the PS-I complex when immobilized on ZnO nanowires. Each 1 cm × 1 cm ZnO nanowire chip covered in PS-I (drops standardized to contain a total of 2.9 μg of protein) was placed on a custom made Teflon holder and cooled under liquid nitrogen (−196.15°C) in a cryostat with glass windows at right angles. Fluorescence was excited optically using a 408 nm laser incident at a −45° angle to the normal to the chip surface. Steady-state emission spectra were recorded using a CCD spectrometer (slit width 20 μm) with an optical fiber input oriented +45° to the normal thus detecting at a right angle from the excitation beam. The fluorescence intensity of each sample was qualitatively normalized and the peaks were found to be identical to those of native PS-I (**Fig. 2c**), as expected if no structural changes resulted from the exchange reaction or immobilization on the ZnO nanowires.

Fabrication of sealed solar cells, current-voltage (IV) and control measurements. Devices (**Fig 1**) were made by allowing a 40 μL drop of PS-I solution to air dry at room temperature on two different nanostructured semiconducting electrodes: a TiO_2 of 60 nm average pore size, 3.8 μm film thickness, roughness factor: ρTiO_2 ~200 (i.e. surface area increases by x50 per μm of film thickness) fabricated as described previously[13] **(Fig 3a)** and a mat of 3 μm tall, ZnO nanowires (grown on Zn-nanoparticle-seeded ITO-glass as described elsewhere[1]) with ρZnO ~30 **(Fig 3b)**. Cells were sealed with 40 μm-thick heat-treated Syrlyn gaskets and Z813 Co(II)/Co(III) electrolyte[14] composed of:

0.5 M Co(Ophen)3(bis(trifluoromethanesulfonyl)imide)$_2$
0.05M Co(Ophen)$_3$(bis(trifluoromethanesulfonyl)imide)$_3$
0.2 M $LiClO_4$ dissolved in a 60%Ethylene Carbonate and 40% acetonitrile (v/v) solvent, which was introduced by capillary action. Platinum-coated, fluorine-doped tin-oxide (FTO) glass was used as the counter electrode. In all cases, photomasks of 0.159 cm^2 where used and IV curves, J_{sc}^{Norm} and total power were normalized to this area. All measurements were performed using a continuously thermopile-calibrated solar simulator with neutral density filters as described in detail by Ito *et al.*[13]. 60 devices total were tested, the results reported in **Fig 4** belong to individual devices exhibiting typical behavior, not averages over many devices. The error bars in all IV curves are included in the plots but are smaller than the size of the data point markers. Control devices made with TiO_2 and electrolyte but containing no PS-I and exposed to full sunlight (including UV) gave P_{out} 28 μW/cm^2, with 277 μA/cm^2 I_{sc} and 257 mV V_{oc} with a fill factor of 0.39. It was impossible to obtain IPCE curves of control unsensitized devices due to very low currents, as expected (see supplemental materials).

PS-I Purification. Our PS-I was identical to that used in Iwuchukwu *et al.*[11]. Briefly, PS-I was extracted from the thylakoid membranes of the thermophilic cyanobacteria *T. elongatus*. Bacteria were grown in 2 L airlift fermenters (Bethesda Research Labs, Bethesda MD) to late log phase at 56°C. Bacterial growth was followed by incubation with 0.25% (w/v) lysozyme for 2 hours at 37°C under gentle agitation. Cells were lysed with the French press; unlysed cells were removed at 3,000 x g for 5 min and membranes were collected at 20,000 RPM. The membranes were washed and solubilized as in Fromme and Witt[20] with the exception that in the final wash 3 M NaBr was used. Then the supernatant was loaded on a 10-30% linear sucrose gradient (20 mM MES pH 7.0, 10 mM $MgCl_2$, 10 mM CaC_{l2} and 0.3% w/v n-dodecyl-b-D-maltopyranoside (DDM), for 16 hours at 24,000 RPM. The lower green band was collected (see Fig. 2 of Iwuchukwu *et al.*[11]), pooled and stored at –20°C. Purity was confirmed by Tris-tricine SDS-PAGE gel electrophoresis. The chlorophyll content of PS-I was measured as described previously[21].

1. Kiley, P. *et al.* Self-assembling peptide detergents stabilize isolated photosystem-I on a dry surface for an extended time. *PLoS Biol.* **3**, 1181–1186 (2005).
2. Collini, E. *et al.* Coherently wired light-harvesting photosynthetic marine algae at ambient temperature. *Nature* **463**, 644–647 (2010).
3. Editorial Live Wires. *Nature Nanotechnology* **1**, 79 (2006).
4. LaVan, D. A. & Cha, J. N. Approaches for biological and biomimetic energy conversion. *PNAS* **103**, 5251–5255 (2006).
5. Das, R. *et al.* Integration of photosynthetic protein molecular complexes in solid-state electronic devices. *Nano Letters* **4**, 1079–1083 (2004).
6. Trammell, S. A., Wang, L., Zullo, J. M., Shashidhar, R. & Lebedev, N. Orientated binding of photosynthetic reaction centers on gold using Ni-NTA self-assembled monolayers. *Biosensors & Bioelectronics* **19**, 1649–1655 (2004).
7. Trammell, S. A., Spano, A., Price, R. & Lebedev, N. Effect of protein orientation on electron transfer between photosynthetic reaction centers and carbon electrodes. *Biosensors and Bioelectronics* **21**, 1023–1028 (2006).
8. Carmeli, I., Frolov, L., Carmeli, C. & Richter, S. Photovoltaic activity of photosystem I-based self-assembled monolayer. *J. Am. Chem. Soc.* **129**, 12352–12353 (2007).
9. Grätzel, M. Photoelectrochemical Cells. *Nature* **414**, 338-344 (2001).
10. Kjærgaard, K., Sorensen, J. K., Schembri, M. A. & Klemm, P. Sequestration of zinc oxide by fimbrial designer chelators. *Appl. Env. Microbiol.* **66**, 10–14 (2000).
11. Iwuchukwu, I., J. *et al.* Self-organized photosynthetic nanoparticle for cell-free hydrogen production. *Nature Nanotechnology* **5** (2009).
12. Matsumoto, K., Vaughn, M., Bruce, B. D., Koutsopoulos, S. & Zhang, S. Designer Peptide Surfactants Stabilize Functional Photosystem-I Membrane Complex in Aqueous Solution for Extended Time. *J. Phys. Chem. B* **113**, 75–83 (2008).
13. Ito, S. *et al.* Fabrication of screen-printing pastes from TiO_2 powders for dye-sensitised solar cells. *Prog. Photovoltaics* **15**, 603–612 (2007).
14. Herve-Nusbaumer, Zakeeruddin, S. M., Moser, J.-E. & Graetzel, M. An alternative efficient redox couple for the dye-sensitized solar cell system. *Chem. Eur. J.* **9**, 3756–3763 (2003).
15. Law, M., Greene, L. E., Johnson, J. C., Saykally, R. & Yang, P. Nanowire dye-sensitized solar cells. *Nature Materials* **4**, 455–458 (2005).
16. Xu, F. *et al.* Simple approach to highly oriented ZnO nanowire arrays: large scale growth, photoluminescence and photocatalytic properties. *Nanotechnology* **17**, 588–594 (2006).
17. Kay, A. & Graetzel, M. Artificial Photosynthesis. 1. Photosensitization of TiO_2 solar Cells with chlorophyll derivatives and related natural porphyrins. *J. Phys. Chem. B* **97**, 6272–6277 (1993).
18. Butler, D. Thin Films: ready for their close-up? *Nature* **454**, 558–559 (2008).
19. Liu, J., Lu, J., Zhao, X., Lu, J. & Cui, Z. Separation of glucose oxidase and catalase using ultrafiltration with 300-kDa polyethersulfone membranes. *Journal of Membrane Science* **299**, 222–228 (2007).
20. Fromme, P. & Witt, H. T. Improved isolation and crystallization of Photosystem I for structural analysis. *Biochimica Et Biophysica Acta-Bioenergetics* **1365**, 175–184 (1998).

21. Demarsac, N. T. & Houmard, J. Complementary Chromatic Adaptation - Physiological Conditions and Action Spectra. *Methods in Enzymology* **167**, 318–328 (1988).
22. Lundell, D. J., Glazer, A. N., Melis, A. & Malkin, R. Characterization of a cyanobacterial photosystem-I complex. *The Journal of Biological Chemistry* **260**, 646–654 (1985).

Acknowledgements

We thank the Intel Corporation for their unrestricted gift partially seed-funding this work. LK gratefully acknowledges her fellowship by the Knut and Alice Wallenberg foundation. SZ gratefully acknowledges the John Simon Guggenheim Foundation for his Guggenheim Fellowship to pursue this research. We are grateful to Sloan Kulper for creating panels c, d & e of Figure 3. We are indebted to S. M. Zakeerrudin, Jun-Ho Yum, Peter Chen and Jiang Liu for their assistance. BB and SZ were partially supported from an NSF NIRT award. BB was partially supported from a gift from the Gibson Family Foundation.

Author contributions

AM, BB and SZ wrote the main manuscript text. AM, KM, LK, DY, MV, MN, BB performed the experiments, AM, KM, LK, MV, BB prepared figures 1–4. All authors reviewed the manuscript.

Additional information

Supplementary Information accompanies this paper at http://www.nature.com/scientificreports

Competing financial interests: The authors declare no competing financial interests

How to cite this article: Mershin, A. *et al*. Self-assembled photosystem-I biophotovoltaics on nanostructured TiO_2 and ZnO. *Sci. Rep.* **2**, 234; DOI:10.1038/srep00234 (2012).